Evolution of groups of gravity waves with moderate to high steepness

Ming-Yang Su

Citation: Physics of Fluids **25**, 2167 (1982); doi: 10.1063/1.863708
View online: http://dx.doi.org/10.1063/1.863708
View Table of Contents: http://scitation.aip.org/content/aip/journal/pof1/25/12?ver=pdfcov
Published by the AIP Publishing

Evolution of groups of gravity waves with moderate to high steepness

Ming-Yang Su
Naval Ocean Research and Development Activity, NSTL Station, Mississippi 39529

(Received 2 March 1982; accepted 8 September 1982)

Experimental measurements of evolution of a deep-water wave group are described. Wave groups are found to change rapidly over a few tens of wavelengths when the initial steepness $0.09 \leqslant a_0 k_0 \leqslant 0.28$. The transition creates envelope solitons composed of waves with smaller steepness and lower carrier frequency than the initial state. The carrier frequencies of the envelope solitons can be downshifted as much as 25%. The transition process is irreversible, but does not lead to total randomness.

I. INTRODUCTION

The ubiquitous presence of wave groups manifesting as orderly, phase-locked variation of adjacent waves has long been noticed in the wind-generated gravity waves in the ocean.[1-3] Current increasing interest in wave groupiness arises for several reasons: (1) its practical relevance to the response of marine structures and ships[4-5]; (2) its importance in estimating statistical properties such as wave spectra and correlation functions,[6-7] and (3) its important role in nonlinear instabilities and evolution of finite-amplitude surface waves.[8-10] The subject of this paper belongs to the last category.

Zakharov and Shabat[11] showed that the nonlinear Schrödinger equation can be solved exactly as an initial value problem for a finite-length wave packet with sufficiently small wave steepness. As far as our present investigation is concerned, their most important theoretical prediction is that the initial wave packet will evolve into a number of envelope solitons and an oscillatory tail, with the number of envelope solitons formed proportional to the product of the initial wave steepness and the length of the wave packet. These predictions have been experimentally verified by Yuen and Lake[10] for small steepness $a_0 k_0 \leqslant 0.1$, where a_0 and k_0 are initial wave amplitude and wavenumber. It should be noted that the derivation of the nonlinear Schrödinger equation is based on three assumptions: (1) weak nonlinearity and thus small wave steepness, (2) existence of a constant carrier frequency, and (3) slow variations of wave amplitude and phase. The experimental verification by Yuen and Lake are also restricted to the cases with small initial steepness.

The objective of the paper is to provide experimental findings on the evolution of wave packets containing from 5–30 waves, with an initial steepness range of $0.1 \leqslant a_0 k_0 \leqslant 0.28$. A new property is shown that of a downshift in the carrier frequency of envelope solitons. Frequency downshift for continuous wave trains with $a_0 k_0 > 0.23$ has been reported, first by Lake *et al.*,[9] and subsequently by Melville[12] for $0.21 \leqslant a_0 k_0 \leqslant 0.28$. Our finding of a frequency downshift during short wave packet evolution, for waves with initial steepness as low as $a_0 k_0 = 0.1$, is significant, not only to demonstrate the limitations of the Zakharov–Shabat theory, but also for evidencing a new transfer of energy from higher- to lower-frequency modes. This instability-induced energy transfer appears to have a higher probability of realization in nature than the much weaker resonant interactions among quartets of waves.[13-14]

In Sec. II we present experimental observations of the transition of wave packets into envelope solitons and subsequent interactions. These observations also show that the evolution of longer wave packets is more complex than that of shorter wave packets.

II. EXPERIMENTAL RESULTS

The experiments for this study were conducted in a tow tank $3.7 \times 3.7 \times 137$ m. The wavemaker is a plunger-type, and the profile of its forward face approximates a hyperbola. The wave height gauges are of the capacitance type. More detailed descriptions of the experimental facility, method, and data analysis can be found in Su *et al.*[15] We have chosen four values of initial wave steepness $a_0 k_0$ from 0.09–0.28 and four values for the number of waves per packet, N, which ranged from 5–20 waves of the same wave height. The number of waves are counted in the time domain as the waves pass a fixed wave gauge, rather than in the spatial domain. Thus, sixteen different initial conditions were used in the experiment and are summarized in Table I.

We shall present the experimental results in the order of the formation of envelope solitons, the transition of wave packets, the corresponding evolution of power spectra, and the energy dissipation through wave breaking.

A. Formation of envelope solitons

Figures 1 through 5 show typical time records of surface displacements during the wave evolution, measured at eight stations with increasing distance x from the wavemaker. As shown in Fig. 1 ($a_0 k_0 = 0.09$, $N = 5$), the wave packet continues to increase its length and decrease its maximal height from $x = 24.4$ m to $x = 106.7$m. No stable envelope soliton is found in this case. It is also noted that small-amplitude, lower-frequency components disperse in front of the leading edge of the wave packet, while a higher-frequency tail occurs behind the packet. In Fig. 2 (with $a_0 k_0 = 0.09$, $f_0 = 0.96$ Hz, $N = 10$) the largest energy-containing portion of the wave packet retains its shape and size consistently from $x = 61.0$ m to $x = 106.7$m and may be regarded as an envelope soliton. The carrier frequency of the envelope soliton is found to be the same as the initial carrier frequency.

TABLE I. Numbers of envelope solitons.

		$N=5$	$N=10$	$N=15$	$N=20$
$a_0k_0=0.09$	$N_{S,E}$	0	1	2	2
	$N_{S,T}$	0.64	1.27	1.90	2.55
$a_0k_0=0.15$	$N_{S,E}$	1	2	3	3
	$N_{S,T}$	1.06	2.12	3.18	4.24
$a_0k_0=0.22$	$N_{S,E}$	2	3	4	5
	$N_{S,T}$	1.56	3.11	4.67	6.22
$a_0k_0=0.28$	$N_{S,E}$	2	3	5	7
	$N_{S,T}$	1.98	3.96	5.94	7.92

Several much smaller waves proceed and follow the envelope soliton.

Figure 3 ($a_0k_0=0.15, f_0=1.15$ Hz, $N=10$) shows the formation of two envelope solitons at $x=61.0$ m, becoming almost completely separate at $x=106.7$ m. The leading envelope soliton is larger in amplitude and has a lower carrier frequency ($f_1=1.0$ Hz) than the trailing envelope soliton; the latter has the same carrier frequency as the original f_0. As in the previous case, some much smaller wave groups proceed and trail these two envelope solitons.

In Fig. 4 ($a_0k_0=0.22, f_0=1.3$ Hz, $N=20$) we note up to five envelope solitons formed by $x=106.7$ m with the middle (third from the right) envelope soliton still in the stage of development. The maximum height of the envelope of these solitons is noted to decrease approximately linearly from the (first) leading envelope soliton to the (last) trailing

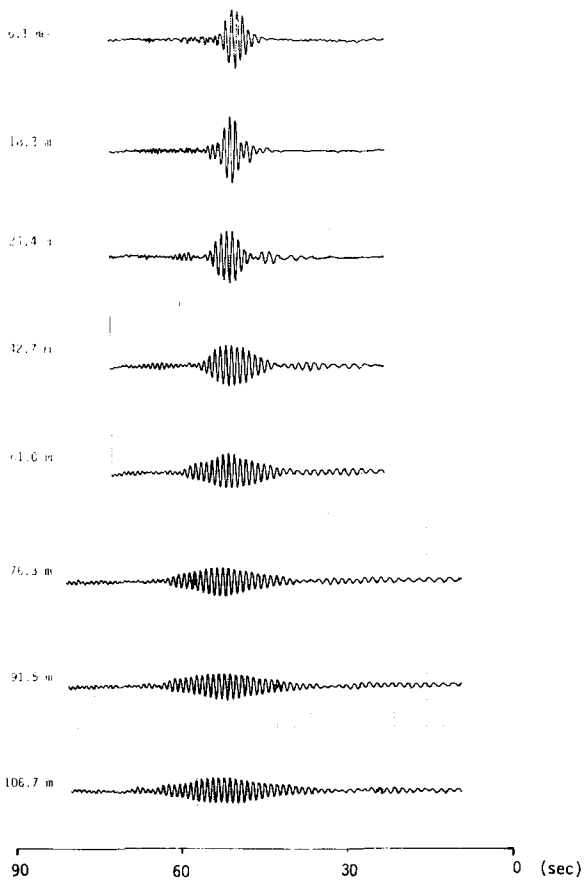

FIG. 1. The evolution of a wave packet with $a_0k_0=0.09$, $f_0=0.96$ Hz, $N=5$. The distances x (in meters) is measured from the wavemaker.

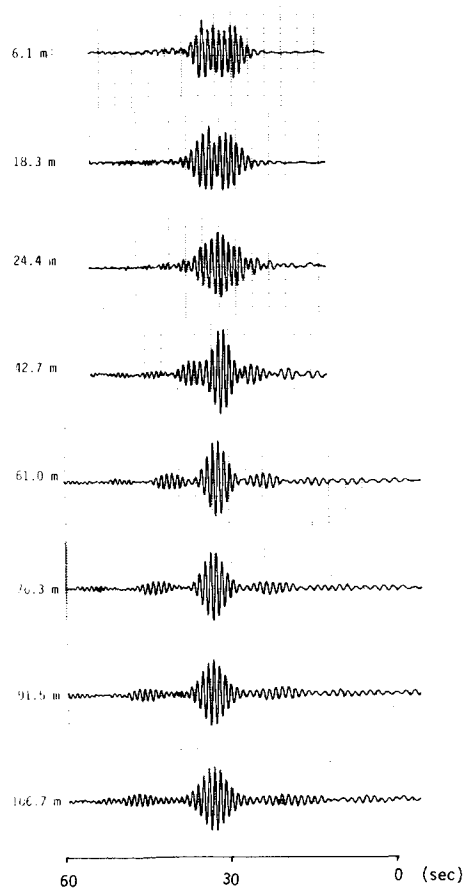

FIG. 2. The evolution of a wave packet with $a_0k_0=0.09$, $f_0=0.96$ Hz, $N=5$.

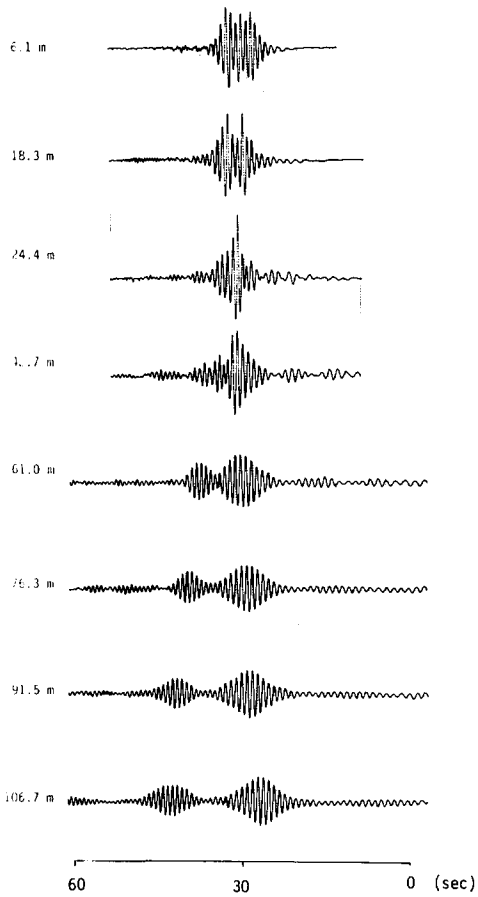

FIG. 3. The evolution of a wave packet with $a_0k_0 = 0.15$, $f = 1.12$ Hz, $N = 10$.

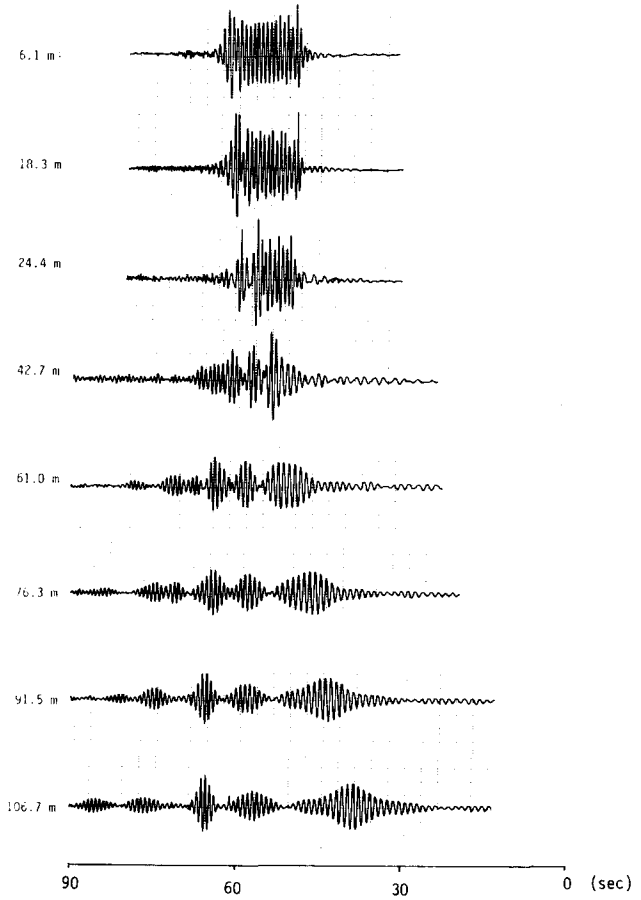

FIG. 4. The evolution of a wave packet with $a_0k_0 = 0.22$, $f_0 = 1.34$ Hz, $N = 20$.

one. The carrier frequencies for these envelope solitons, respectively, are $f_1 = 1.0$ Hz, $f_2 = 1.2$ Hz, $f_3 = 1.2$ Hz, $f_4 = 1.34$ Hz, $f_5 = 1.34$ Hz. Thus, the first three carrier frequencies are lower than the carrier frequency of the initial wave packet. The dynamical process involved in the formation of these envelope solitons must be highly nonlinear and complex, since there is an extremely strong envelope modulation from $x = 18.3$ m to $x = 42.7$ m (in Fig. 4). In the wave profile at $x = 24.4$ m, alternate high and low wave crests characterize a subharmonic instability with a perturbation period of two fundamental wave periods. Due to the frequency dispersion, the total length of the wave packet at $x = 106.7$ m is much greater than at $x = 61.0$ m.

Figure 5 ($a_0k_0 = 0.28$, $f_0 = 1.44$ Hz, $\lambda_0 = 0.65$ m, $N = 20$) shows the case with the largest initial wave steepness. The characteristics of evolution are similar to the case in Fig. 4, except that there are more (seven) envelope solitons, and some are developing at $x = 106.7$ m. These envelope solitons in the middle portion of the wave packet again are found to lag in their formation when compared with both the leading and the trailing envelope solitons.

Table I summarizes the experimental results for the 16 initial wave conditions of wave steepness and wave packet size. From the total collection of findings, the average number of envelope solitons formed, $N_{S,E}$ for each initial condition is calculated indicating that $N_{S,E}$ increases monotonically with N or a_0k_0, and varies almost linearly with Na_0k_0.

B. Transition process of wave packets

We note in Figs. 4 and 5 that the modulation, which ultimately forms envelope solitons, seems to complete faster at the leading and trailing ends of a wave packet. In order to learn more of this tendency, we conducted experiments with a longer wave packet, $N = 60$, and a fixed carrier frequency of $f_0 = 1.24$ Hz, but with a_0k_0 varying from 0.09 to 0.22. The temporal records of the surface displacement for three such cases are shown in Figs. 6–8.

In Fig. 6 ($N = 60$, $a_0k_0 = 0.09$, $f_0 = 1.24$ Hz) the modulation of the amplitude envelope is seen to be almost symmetric with respect to the center of the wave packet. The envelope modulation is smaller in the middle portion of the wave packet compared with the leading and trailing portions. At $x = 106.7$ m, six envelope solitons, composed of four almost completely formed and two incompletely formed, are found to be about the same size, in clear contrast to the large variation in sizes observed in Figs. 4 and 5 for smaller N, and larger a_0k_0. Comparing Fig. 6 and Fig. 1 ($a_0k_0 = 0.09$ for both) we conclude that the latter case simply contains either too few waves or, equivalently, too little energy and momentum to be able to form an envelope soliton at that frequency.

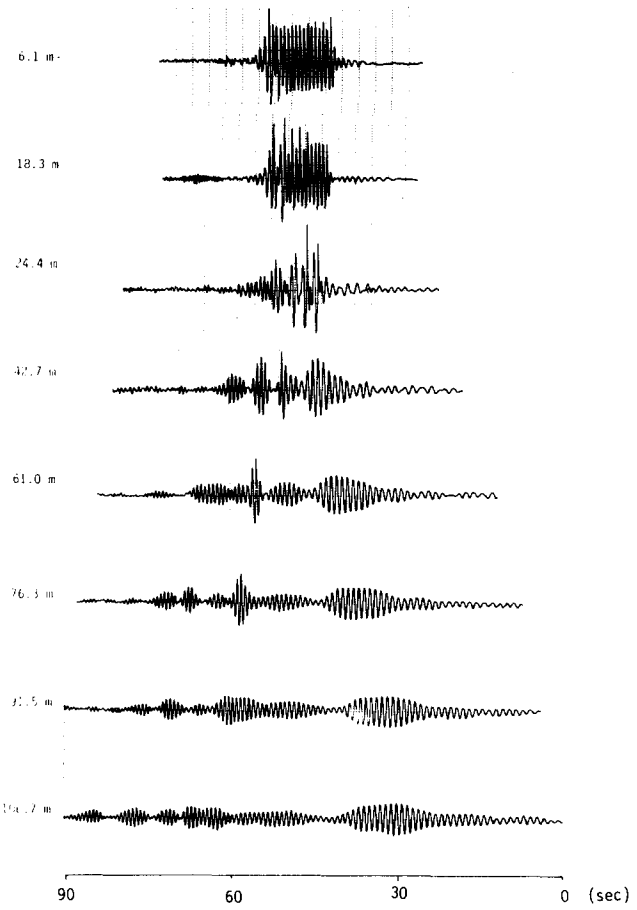

FIG. 5. The evolution of a wave packet with $a_0k_0 = 0.28$, $f_0 = 1.49$ Hz, $N = 20$.

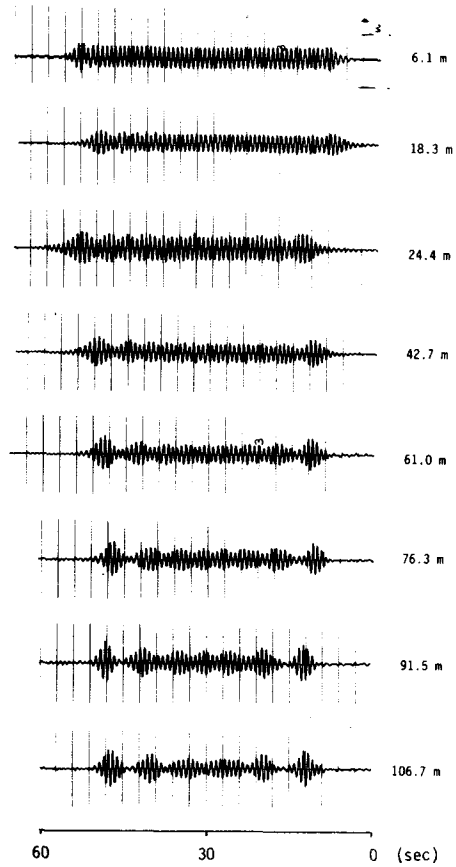

FIG. 6. The evolution of a wave packet with $a_0k_0 = 0.09$, $f_0 = 1.24$ Hz, $N = 60$.

In Fig. 7 ($N = 60$, $a_0k_0 = 0.15$, $f_0 = 1.24$ Hz) which has a larger steepness than in Fig. 6, we observe a similar symmetric modulation for the entire wave packet from $x = 6.1$ m to $x = 42.7$ m. A small amount of contraction (about 5%) of the total length (in time) of the wave packet is also noted in the same period of wave evolution. However, from $x = 42.7$ m to $x = 91.5$ m, we see a stronger modulation in the leading portion than in the trailing portion. The feature shows progressively more intensity as x increases. Finally, at the last station, $x = 106.7$ m, a single large modulation again occurs at around 40 seconds from the leading end (compare the corresponding portion at $x = 91.5$ m to see the difference).

In Fig. 8 (with $a_0k_0 = 0.205$, $f_0 = 1.24$ Hz, $N = 60$) similar characteristics of the envelope modulation can be discerned, with the main difference being stronger modulation for the initially steeper waves. Note that no envelope soliton can be seen even at $x = 106.7$ m for both cases in Figs. 7 and 8. In contrast, envelope solitons are observed clearly in Fig. 3 ($a_0k_0 = 0.15$) and Fig. 4 ($a_0k_0 = 0.22$), with a shorter wave packet ($N = 10$). Finally, we note that the largest waves at $x = 61.0$ m and $x = 76.3$ m in Fig. 8 are larger than any waves from $x = 6.1$ m to $x = 42.7$ m. The above asymmetric modulations observed in Figs. 7 and 8, in comparison to the symmetric modulations in Fig. 6, we attribute to multiple collisions (interactions) of different evolutionary stages of envelope solitons with different carrier frequencies; those

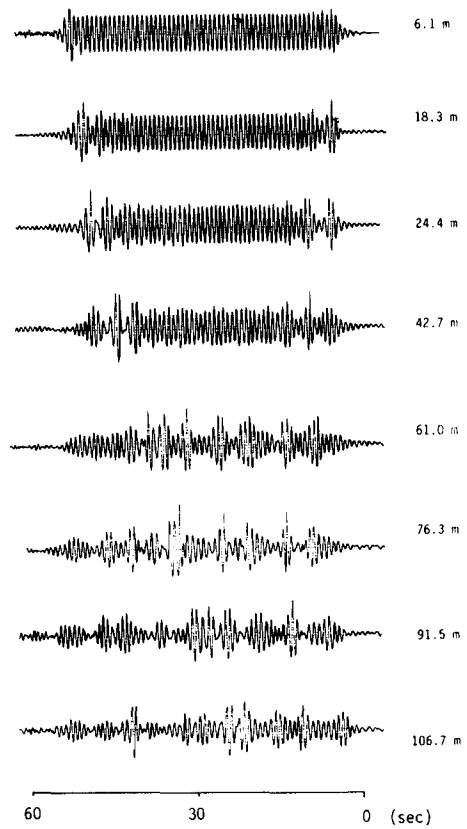

FIG. 7. The evolution of a wave packet with $a_0k_0 = 0.15$, $f_0 = 1.24$ Hz, $N = 60$.

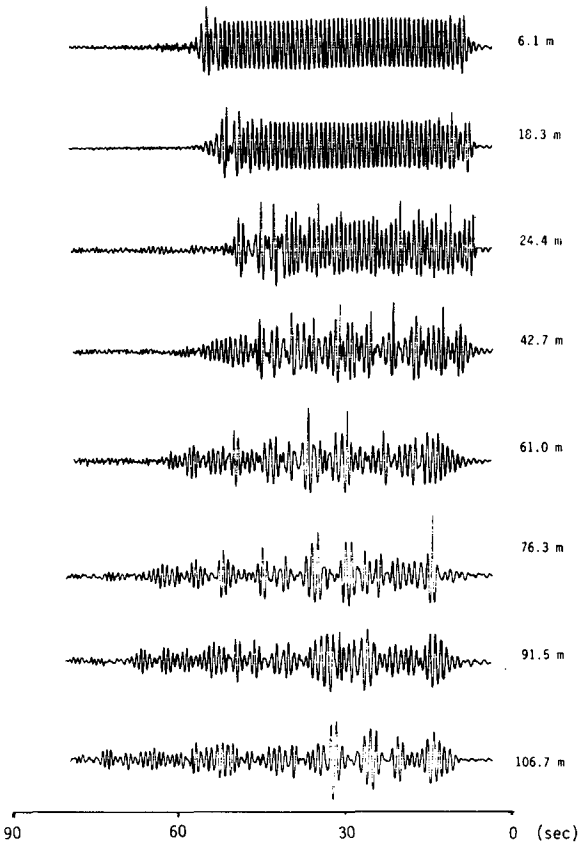

FIG. 8. The evolution of a wave packet with $a_0k_0 = 0.205$, $f_0 = 1.24$ Hz, and $N = 60$.

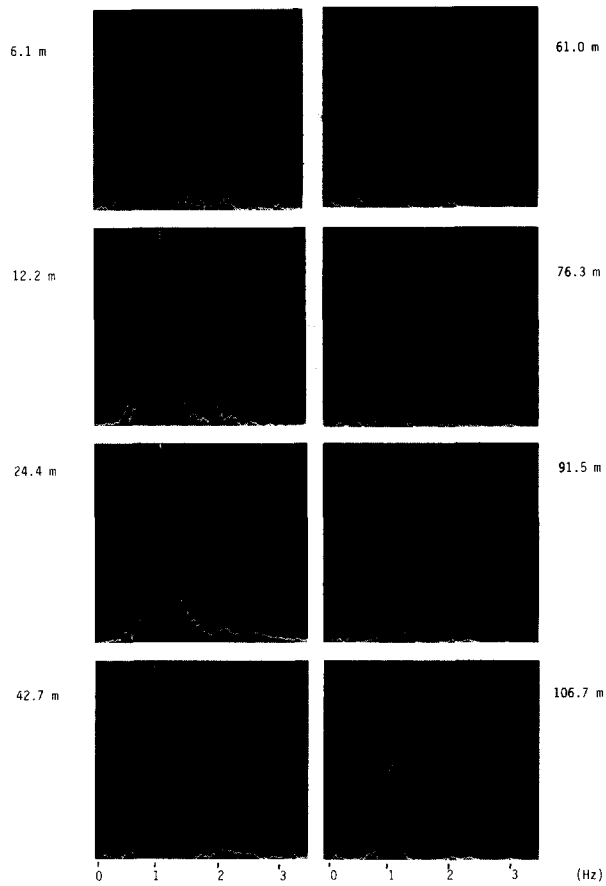

FIG. 9. The evolution of power spectra corresponding to the evolution in Fig. 3.

envelope solitons with lower carrier frequencies move at greater group velocities and, consequently, run into preceeding envelope solitons with higher carrier frequencies. This type of nonlinear collision results in relative position and phase changes. In contrast, the case with small $a_0k_0 = 0.09$ (Fig. 6) can be said to experience no collision of envelope solitons up to the last station at $x = 106.7$ m.

C. Frequency downshift in carrier frequency

In order to examine more quantitatively the evolution of wave packets in the frequency domain in general and the phenomenon of frequency downshift in particular, we present in Figs. 9–11 three sets of surface displacement power spectra corresponding to the cases in Figs. 3–5, respectively. A comparison among these spectral evolutions reveals several common characteristics. We shall use Figs. 4 and 10 with $a_0k_0 = 0.22$ as a typical example to elucidate these characteristics, and leave the other two pairs for interested readers to confirm their commonality. In Fig. 10 at $x = 6.1$ m, the single narrow peak at $f_0 = 1.3$ Hz is the initial carrier frequency of the wave packet. From $x = 18.3$ m to $x = 61.0$ m, the f_0 peak first increases and then decreases steadily, while a secondary peak $\bar{f} = 1.0$ Hz forms at the expense of the carrier peak. Beyond $x = 61.0$ m, we find the growth of a third peak $\bar{\bar{f}} = 1.2$ Hz. The appearance of these three narrow spectral peaks with $f_0 > \bar{f} > \bar{\bar{f}}$, in both their frequencies and the order of their appearance (with respect to the distance from the wavemaker), corresponds very well with our earlier description of the formation of the five envelope solitons in Fig. 4; i.e.,

$$f_1 = \bar{\bar{f}} < f_2 = f_3 = \bar{f} < f_4 = f_5 = f_0.$$

Next, we shall compute the ratio of the largest frequency shift with respect to the initial carrier frequency δ as

$$\delta = (f_0 - f)/f_0. \tag{1}$$

For Fig. 9 with $a_0k_0 = 0.15$,

$$\delta = (1.14 - 1.0)/1.14 = 0.14.$$

For Fig. 10 with $a_0k_0 = 0.22$,

$$\delta = (1.3 - 1.0)/1.3 = 0.23.$$

For Fig. 11 with $a_0k_0 = 0.28$,

$$\delta = (1.42 - 1.02)/1.42 = 0.28.$$

The above values suggest that

$$\delta \simeq a_0k_0. \tag{2}$$

That is, there is a close linear relationship between the largest frequency shift and the initial wave steepness. All the other carrier frequencies of envelope solitons formed lie between f_0 and $\bar{f} = f_0(1 - \delta)$.

D. Wave breaking and energy dissipation

The evolution of wave packets of steepness $a_0k_0 \gtrsim 0.14$ is found to involve a varying degree of wave breaking, which

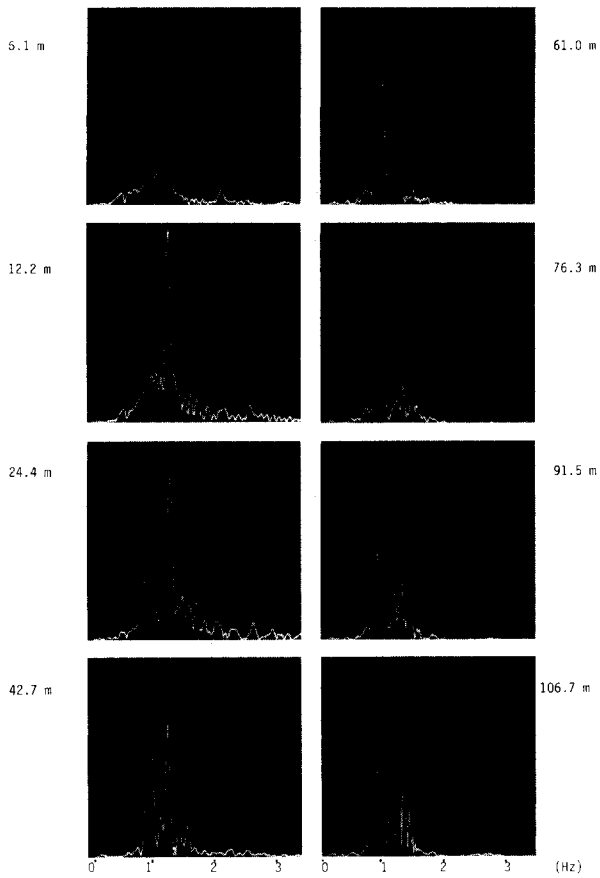

FIG. 10. The evolution of power spectra corresponding to the evolution in Fig. 4.

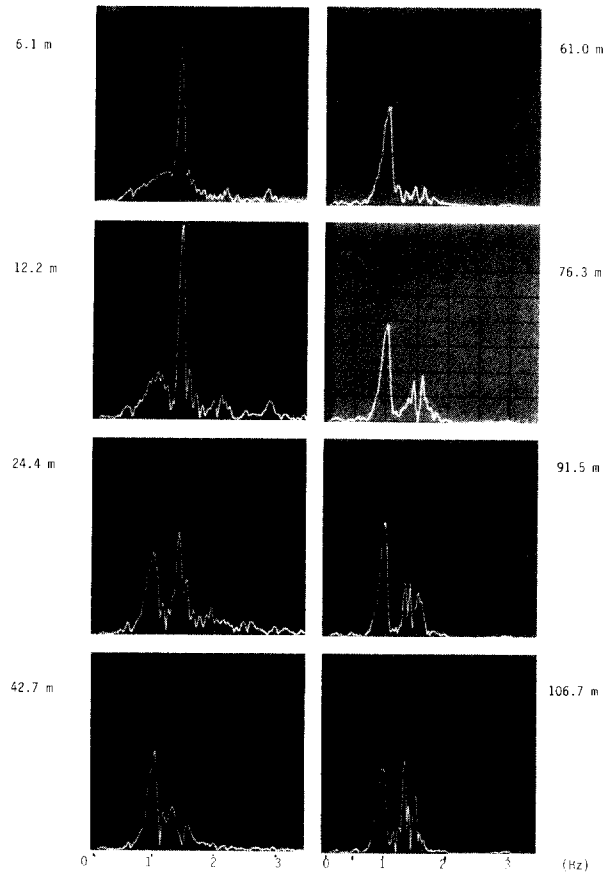

FIG. 11. The evolution of power spectra corresponding to the evolution in Fig. 5.

depends also on the size of waves in the packet. Direct observation on the energy dissipation during the evolution of wave packets (other than the losses due to surface tension and viscous effects on the side walls of the wave tank) may be summarized below.

(a) From $x = 10\lambda_0$ to $20\lambda_0$, intense two-dimensional breaking always occurs at the trailing wave of the packet. The intensity of the trailing breaker decreases with N.

(b) From $x = 15\lambda_0$ to $25\lambda_0$, the leading wave of the packet often develops into a number of regularly spaced, three-dimensional, crescent-shaped breaking waves. The crestwise separation of these breakers is about $0.8\lambda_0$ and the occurrence and intensity of this type of breaking increases with N. Further, as N increases, three-dimensional breakers occur in the middle of the wave packet for $a_0k_0 \gtrsim 0.2$. The underlying cause for the three-dimensional breaking have been discussed by McLean *et al.*[16] and Su.[17]

(c) From $x = 20\lambda_0$ to $45\lambda_0$, the largest waves present in the wave packet often develop into two-dimensional (long-crested) spilling-type breaking waves which generate continuous turbulent wakes near the water surface entraining air bubbles. The intensity of the spilling breakers decreases with N.

From the above summary, we could further appreciate the complexity of the nonlinear evolution of wave packets of moderate to large steepness.

III. COMPARISONS OF EXPERIMENTS WITH THEORY

A. The Zakharov and Shabat (Z–S) theory

Based on the nonlinear Schrödinger equation for weakly nonlinear, dispersive gravity waves,

$$i\left(\frac{\delta A}{\delta t} + \frac{1}{2}\frac{w_0}{k_0}\frac{\delta A}{\delta x}\right) - \frac{w_0}{8k^2}\frac{\delta^2 A}{\delta x^2} - \frac{1}{2}w_0 k_0^2 |A|^2 A = 0, \tag{3}$$

where $i = \sqrt{-1}$, $A = a(x, t)e^{i\theta}(x, t)$ is the complex amplitude with slowly varying real amplitude $a(x, t)$ and phase $\theta(x, t)$, Zakharov and Shabat[11] solved the initial-value problem for a wave packet whose amplitude approaches zero sufficiently rapidly as $|x| \to \infty$. It should be stressed that the Z–S solution, as constrained by the underlying assumption in the derivation of the nonlinear Schrödinger equation, demands specifically constancy of the carrier frequency w_0 and wavenumber k_0 during the entire evolutionary process. These two parameters are related by the linear dispersion relationship $(2\pi w_0)^2 = gk_0$. So far as our purpose here is concerned, the Z–S theory predicts that:

(a) The initial wave packet will evolve asymptotically (i.e., $t \to \infty$) into a number of envelope solitons and an oscillatory tail with relatively small amplitude.

(b) The envelope soliton is a permanent, progressive wave solution with an envelope shape a function of sech, that

have the remarkable property that they will survive mutual collisions without change in their shapes, except for possible change of phase and relative position.

(c) The time scale of the formation of these envelope solitons is proportional to the size N of the wave packet, and inversely proportional to the wave steepness a_0k_0.

(d) The number of envelope solitons formed $N_{S,T}$ is estimated to be

$$N_{S,T} = \frac{1}{\pi}\int_0^\infty \sqrt{2}\, k_0^2 a_0 q(x)dx, \tag{4}$$

where $A(x, 0) = a_0q(x)$ with $0 \leqslant q(x) \leqslant 1$. In particular, for $q(x) = 1$, $0 < x < L_0$ and $L_0 = (\frac{1}{2}N)\lambda_0 = (\pi/k_0)N$, we have

$$N_{S,T} = \sqrt{2}\, a_0k_0N. \tag{5}$$

The particular case $q(x) = 1$ gives the approximate shape of the wave packets used in our experiments in Sec. II. The reason for using $L_0 = (1/2)N\lambda_0$ rather than $L_0 = N\lambda_0$, is that N is defined as the number of waves in the initial wave packet in the *temporal domain*, rather than the spatial domain, and the group velocity of gravity waves is about one-half of the phase velocity. Thus, there is only one-half as many waves in a wave packet in the space domain as in the time domain.[18] The first three predictions (a), (b), and (c) compare well with our experiment and Yuen and Lake.[10]

For small $a_0k_0 < 0.1$, our experiments confirm Yuen and Lake[10] of the (d) prediction. However, for $a_0k_0 > 0.1$, the theoretical prediction deviates more from our experiments as a_0k_0 and N become larger. In Table I, we list the $N_{S,T}$ computed by Eq. (5) and the experimentally observed $N_{S,E}$. We find that $N_{S,T}$ agrees welll with $N_{S,E}$, if

$$(a_0k_0)N \lesssim 5.5. \tag{6}$$

For $a_0k_0N > 5.5$, $N_{S,T}$ is found to be greater than $N_{S,E}$. It should be noted that for the case with $a_0k_0 = 0.09$ and $N = 5$, yielding $N_{S,T} = 0.64 < 1$, no stable envelope soliton was observed in the experiment (Fig. 1) which was consistent with the theoretical prediction. It appears that there exists a lower bound $a_0k_0\,N = 1/\sqrt{2}$, below which the wave packet cannot maintain a balance between the dispersive effect and nonlinearity; such balance is needed to create envelope solitons.

B. Benjamin–Feir instability

The modulation instability of a continuous wave train of weakly nonlinear waves was first shown by Benjamin and Feir[19,20] to be related to subharmonic side-band instability. This type of instability for finite-amplitude waves was computed more accurately by Longuet–Higgins[21] by a two-dimensional normal mode analysis, and by McLean *et al.*[16] by numerical solution of a continuously perturbed, three-dimensional, water wave equation. All these analyses are based on *linear* perturbation methods. As such, their computations are applicable for only initial growth of the instabilities. For our purpose here, the main prediction of the Benjamin–Feir instability is that the wave train is unstable to perturbation mode f for

$$f_0(1 - \sqrt{2}\, a_0k_0) \leqslant f \leqslant f_0(1 + \sqrt{2}\, a_0k_0), \tag{7}$$

and that the most unstable (or fastest growing) perturbation modes are

$$f = f_0\,(1 \mp a_0k_0). \tag{8}$$

The above sideband instability may account for two observed features noted in Sec. II. The first is the rapid growth of the spectral peak $\bar{f} = f_0(1 - \delta) = f_0(1 - a_0k_0)$ in the early stage of spectral evolution (see Figs. 9 and 11) from $x = 6.1$ m to $x = 61.0$ m.

The second feature is related to the approximately equal rate of modulations of the leading and trailing portions of a wave packet (see Figs. 6 and 7). It is reasonable to assert that at $t = 0$ there is a larger amount of subharmonic perturbations available for initiating the side-band instability at the ends of the wave packet due to the rapid decrease to zero of the amplitude envelope at these portions in comparison with the relatively uniform envelope shape at the middle of the wave packet. Further, once the instability starts to grow, the leading and trailing portions behave as two relatively independent wave packets that are much shorter than the entire wave packet. It then follows from prediction (d) of the Z–S theory that the envelope solitons should be easier (and thus earlier) to form at the ends of a wave packet.

C. Frequency downshift

The most important discrepancy between our experimental results and the Zakharov and Shabat theory is the fact that for the experimental wave packets with $a_0k_0 > 0.1$, the leading envelope solitons have carrier frequencies lower than the initial fundamental frequency of the wave packet. This phenomenon is inconsistent with the underlying assumption of constancy of the carrier frequency in the derivation of the nonlinear Schrödinger equation, and consequently, cannot be predicted by the equation.[9] No satisfactory explanation on the frequency downshift, which follows the initial instability of Benjamin–Feir type, has been proposed yet, however.

D. Multiple collisions of envelope solitons

The frequency downshift of envelope solitons will lead to a greater group velocity. This fact, in connection with the fact that some envelope solitons form at the trailing portion earlier than at the middle section of the wave packet, naturally results in multiple collisions between envelope solitons. Ultimately, a number of envelope solitons arranged in an order of increasingly higher carrier frequencies will evolve from any given wave packet $a_0k_0\,N > 1/\sqrt{2}$; the envelope soliton with the lowest carrier frequency will be at the lead.

E. Relevance to ocean waves

The prevailing view of random ocean wave field is of a linear composition of Fourier components traveling freely in different directions with different phases. An alternative view may be nonlinear collisions (or interactions) of many envelope solitons of different carrier frequencies traveling at different directions and phases. From the consideration of stability (of wave groups), which controls the existence of any equilibrium solution of any nonlinear dynamical system, the nonlinear viewpoint of random ocean waves consisting

of envelope solitons seems a more appealing physical picture than the classical linear one. One current drawback of the above nonlinear realization is its two-dimensionality of envelope solitons, since field observations indicate that the crestwise lengths of dominant waves are of the order of only a few wavlengths. Real random ocean waves are thus more complex than the nonlinear dynamical picture depicted above.

IV. CONCLUSION

Based on the experimental results for evolution of wave packets of uniform wave heights with initial wave steepness $0.1 < a_0 k_0 \leqslant 0.28$, wave packet size $5 \leqslant N \leqslant 60$, and comparison with existing theories, we draw the following conclusions:

(a) The number of envelope solitons formed, N_S, agrees well with the prediction by Zakharov and Shabat,[11] *i.e.*, $N_S = \sqrt{2}\, a_0 k_0\, N$ for $a_0 k_0\, N < 5.5$; but the Zakharov and Shabat theory overpredicts N_S when the above condition is violated.

(b) The carrier frequencies of the envelope solitons formed lies between the fundamental frequency f_0 and $f = (1 - a_0 k_0) f_0$. The lower the carrier frequency, the larger the amplitude envelope and, thus, the larger the total energy (per unit width) in an envelope soliton.

(c) The cause for the downshift of the carrier frequencies is related to the side-band instability, but cannot be explained by the Zakharov and Shabat theory, which assumes a constant carrier frequency.

(d) The initial stage of the evolution shows an approximately symmetric modulation at the leading and trailing portions. The modulation of these portions grows at a rate faster than at the middle portion of the wave packet.

(e) The combined effect of (c) and (d) leads to multiple collisions between envelope solitons of different carrier frequencies. This chance of collisions increases with N, which, in turn, offers a plausible explanation why distinctively isolated envelope solitons can be observed only in the evolution of a wave packet, but not in the evolution of a continuous wave train of finite steepness. This, ultimately, demonstrates the fundamental importance of the evolution of wave packets in nonlinear wave dynamics.

ACKNOWLEDGMENTS

The author wishes to thank Paul Marler and Richard Myrick for their assistance in conducting the experiments, and to Dr. A. W. Green for helpful suggestions concerning improvement of an earlier manuscript.

[1] K. Nagai, Coastal Eng. Japan **16**, 13 (1973).
[2] J. A. Ewing, J. Geophys. Res. **78**, 1933 (1973).
[3] K. G. Nolte and F. H. Hsu, J. Soc. Petrol. Eng. **22**, 139 (June, 1973).
[4] H. F. Burchorth, Coastal Eng. **2**, 189 (1979).
[5] R. R. Johnson, J. Ploeg, and E. P. D. Mansard, Proceedings of the 16th Coastal Engineering Conference, Hamburg, Germany (1978).
[6] E. Mollo-Christensen and A. Ramamonjisoa, J. Geophys. Res. **83**, 4117 (1978).
[7] W. H. Hui and J. Hamilton, J. Fluid Mech. **93**, 117 (1979).
[8] J. Hamilton and W. H. Hui, J. Geophys. Res. **84**, 4875 (1979).
[9] B. M. Lake, H. C. Yuen, H. Rungaldier, and W. Ferguson, J. Fluid Mech. **83**, 49 (1977).
[10] H. C. Yuen and B. M. Lake, Phys. Fluids **18**, 956 (1975).
[11] V. E. Zakharov and A. B. Shabat, Zh. Eksp. Teor. Fiz. **61**, 118 (1971) [Sov. Phys. JETP **34**, 62 (1972)].
[12] W. K. Melville, J. Fluid Mech. **115**, 165 (1982).
[13] O. M. Phillips, J. Fluid Mech. **9**, 183 (1960).
[14] O. M. Phillips, J. Fluid Mech. **106**, 215 (1981).
[15] M. Y. Su, P. Marler, and R. Myrick, J. Fluid Mech. **124**, 45 (1982).
[16] J. W. McLean, Y. C. Ma, D. U. Martin, P. G. Saffman, and H. C. Yuen, Phys. Rev. Lett. **46**, 817 (1980).
[17] M. Y. Su, J. Fluid Mech. **124**, 73 (1982).
[18] M. S. Longuet-Higgins, J. Fluid Mech. **99**, 705 (1980).
[19] T. B. Benjamin, Proc. R. Soc. London Ser. A **299**, 59 (1967).
[20] T. B. Benjamin and J. E. Feir, J. Fluid Mech. **27**, 417 (1967).
[21] M. S. Longuet-Higgins, Proc. R. Soc. London Ser. A **360**, 489 (1978).